7th International Conference on the Durability of Concrete Structures
20-22 May **2022**
University of Jinan, Jinan, Shandong, China

The transportation of corrosion products in cementitious material under chloride-rich environment

Yuzhou Wang, Haiyu Wang, Yuxi Zhao
Institute of Structural Engineering, Zhejiang University, Hangzhou, China

ABSTRACT

Corrosion products, forming on steel bar in cementitious material, can lead to concrete cracking. Clear the transportation of corrosion products is of great significance to predict corrosion-induced structural deterioration. This study investigates the corrosion products in steel-reinforced concrete specimen. By Raman spectroscopy and SEM method, the chemical constituents and micromorphology of corrosion products at steel-concrete interface as well as those inside the pore of cement paste are investigated. The proportion of corrosion products filling into the cement paste is determined by EDTA titration method. The results reveal that corrosion products diffuse in forms of ion in solution under chloride-rich environment, and the mechanisms of corrosion products filling is explained from physicochemical view.

1.INTRODUCTION

Steel is one of the major causes of the deterioration of reinforced concrete structural durability [1]. Due to the larger volume of corrosion products compared to the original steel, the propagation of steel corrosion could lead to concrete cracking. Corrosion-induced cracking is the stage of great importance for its accelerated influences on corrosion process [2]. However, the time-to-cracking is hard to be predicted for the reason that a portion of corrosion products transport away from steel-concrete interface as liquid-like phase and would not induce any volume expansion [3].

Therefore, its necessary to clear the transportation law of corrosion products in concrete and its corresponding mechanisms to enable the accurate prediction of corrosion-induced cracking in concrete.

Initially in the research field of reinforced concrete structure, it is the filling phenomenon of corrosion products reveal the transportation of corrosion products at steel-concrete interface and surrounding concrete [4]. By using SEM method, a mixed-layer with mortar-like micro-structure was found at the steel-concrete interface, the corresponding location was always called as “porous zone”. The mixed-layer had a thickness of 50 micrometers and was filled by rust particles [5]. Galvanostatic method was used to accelerate steel corrosion in cylindrical concrete specimen, and meanwhile, a high-resolution optical device is fixed to monitor the displacement variation at steel-concrete interface [6]. In the first 3.5 hour, there was no strain caused being detected at steel-concrete interface, indicating that all of the corrosion products filled into the porous zone. X-ray attenuation method was also used to monitor the position of corrosion products after different corrosion time [7]. Due to the differential of attenuation rate of x-ray intensity when passing through different substantial, the corrosion products was found to fill into surrounding concrete within 0.18 mm away from steel-concrete interface.

After confirming the filling phenomenon of corrosion products, some models were also established for quantitatively predicting a specific ratio of corrosion products that filled into porous zone and surrounding concrete. In preceding researches, some simple formulas were proposed to describe the filling capacity of corrosion products [8]. By using galvanostatic method to accelerate steel corrosion in cylindrical concrete specimen. Then, the specimen was cut into large amounts of slices to examine the corrosion products filling in different sections by SEM method. The thickness of corrosion layer and the region filled by corrosion products were measured names as “CL” and “CP”, respectively. By data analysis, a linear relationship was built between “CL” and “CP”. There was also an upper limit of “CP”, which was at most millimeter-level.

On account of the filling phenomenon, some hypotheses were also given to explain the mechanisms of the corrosion products transportation. Some insisted that the corrosion products transportation was corrosion products in solid phase moved by moisture flow in essence [9]. After the corrosion-induced cracks penetrated through the concrete cover, the corrosion products were carried by moisture and flew out of concrete.

Unfortunately, those models and hypotheses were in consistent with the phenomenon observed from reinforced concrete in natural environment. 1000 almost identical, precast reinforced concrete specimen exposed to the North Sea in Scotland more than 60 years were investigated [10]. In some cases, the cross section of steel bar reduced to a

zero cross section whereas only a little irregular black trace was found at corresponding position. Little evidence of rust staining and concrete cracking were shown in reinforced concrete specimen exposed to natural condition. This finding implied that transportation of corrosion products in concrete exposed to natural chloride-rich environment were more complex.

Therefore, in this paper, reinforced mortar blocks exposed to artificial chloride-rich environment and reinforced concrete block exposed to tidal region in marine environment were chosen as research objects. The mortar blocks were destructed and the corrosion products at steel-concrete interface were extracted to investigate the chemical constituents and micromorphology through SEM method. The solution extracted from exposure environment was detected by Raman spectroscopy. The concrete blocks were carefully cut into slices, broke up and ground to particles to titrate the iron content. The corrosion products adhered to steel bar were also dissolved to determine the amount of corrosion products consisting corrosion layer. Combining with the experimental results and physicochemical theory, the mechanisms of corrosion products transportation were explained.

2. EXPERIMENTAL PROGRAMS

2.1 Information of specimen

The experimental programs involved two kinds of specimens, as shown in Table 1. As shown in Figure 1(a), the first kind were sixty-four steel-reinforced mortar blocks consisted of mortar, fine aggregate and cement. Besides, sodium chloride was added in mortar to accelerate the process of chloride ion ingress, and the mass of which is equal to 2% cement contents. In this paper, four of the mortar blocks were investigated. The mix proportion of mortar can be referred to Table 2. The chemical composition of steel bar can be referred to Table 3. The second kind were concrete blocks of Hangzhou Bay Bridge. In this paper, the block named CHCD0-23 was investigated, where C represents the specimen is casted according to standard of pile caps, H represents high-performance concrete, the second C represents the tidal zone, and D0 represent the anti-corrosion precaution applied to steel bar (no anti-corrosion precaution). The mix proportion of concrete can also be referred to Table 2. For both the two types of specimens, only one face was exposed to aggressive environment and the other five faces were coated by anti-corrosion paint.

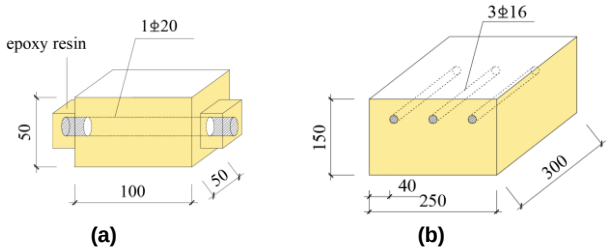

Figure 1. Scheme of specimens(a)mortar block (b)concrete block of HangZhou Bay Bridge

Table 1 Overview of specimens

Specimen label	Type	Size (mm)	Research contents
M-0.5-10	Mortar	40x40x100	Constituents of corrosion products
M-0.65-15		50x50x100	
M-0.5-15		50x50x100	
M-0.5-20		60x60x100	
CHCD0-23	Concrete	150x250x300	Transportation of corrosion products

2.2 Exposure history

After 28-day curing in December 2020, the mortar blocks were put into water-proof polythene box. To prepare 3.5% NaCl solution for simulating the aggressive environment, deionized water was used for preventing the introduction of impurity. Then, each mortar block was carefully put into individual box, the liquid level was just over the upper face of the block. This process lasted for 24 hours and was called as “wet cycle”. Subsequently, the block was taken out with nitrile gloves and put into another empty polythene box. This polythene box was moved into a chamber with constant temperature (25 degrees Celsius) and humidity (RH=50%). This process lasted for 72 hours and was called as

Table 2. Mix proportions of specimens

Specimen label	Consumption of material (kg/m^3)							
	Cement	Slag	Fly ash	Sand	Aggregate	Water	Water reducer	Sodium chloride
M-0.5-10	450	/	/	1350	/	225	/	9 (equal to 2% cement content)
M-0.65-15	450	/	/	1350		292.5	/	
M-0.5-15	450	/	/	1350	/	225	/	
M-0.5-20	450	/	/	1350	/	225	/	
CHCD0-23	162	81	162	779	1032	134	4.86	/

Table 3. Chemical constituents of steel bar

Element	Fe	Mn	Si	S	P	Cu	Ni	Mo
Proportion(%)	98.00	1.10	0.72	0.01	0.02	0.08	0.06	/

"dry cycle". The "wet cycle" and "dry cycle" constitute the 4-day wet-dry cycle. After 9-month cycle, the mortar blocks were taken out and further processed. The concrete block CHCD0-23 were also subjected to "wet-dry cycle" after 28-day curing in March 2013. During the "wet cycle", the block was immersed in 5% NaCl solution for 4 hours. During the "dry cycle", the block was dried in the wind for 44 hours and the temperature was 20 degrees Celsius. After 13-moth cycle, the concrete block was taken out in June 2014 and placed in chloride-free natural environment. In September 2020, the concrete block was taken out and further processed.

2.3 Raman Spectroscopy

The solution (3.5% NaCl dissolved in deionized water) where the mortar blocks had been immersed were not contaminated during the whole wetting-drying cycles. Therefore, the compositional variation of the solution after the wet-dry cycle is directly related with the mass transportation at the interface of specimen and solution. Liquid samples were pipetted from the solution and then stored in a centrifuge tube. Cuvettes were prepared for Raman Spectroscopy to investigate the composition of the solution.

As shown in figure 2a, Confocal Raman Spectroscopy (HORIBA Jobin Yvon XploRA) was used. The liquid sample was put into cuvette. The laser 514.5 nm radiation was used with a power of 50 mW to detect the substance in solution samples. A microscope was used to guide the laser beam and collect the signal from the chosen point of sample.

2.4 Field emission scanning electron microscope

After wet-dry cycles, the mortar blocks were destructed and the steel bars were taken out. Copper knife was used to scrape the corrosion products on the steel bar surface. The corrosion products were collected in a ceramic bowl and dried in oven (90 degrees Celsius, 1 hour). At this temperature, the adsorbed water would lost to evaporation and the chemical composition of corrosion products would not change [11].

The dried corrosion products were scatted on conductive adhesive to make the sample. The sample were firmly stuck and then put into sputter coater (Cressington 108) for spraying process. Then the sample was put into field emission scanning electron microscopy (FE-SEM) to study the microstructure of corrosion products.

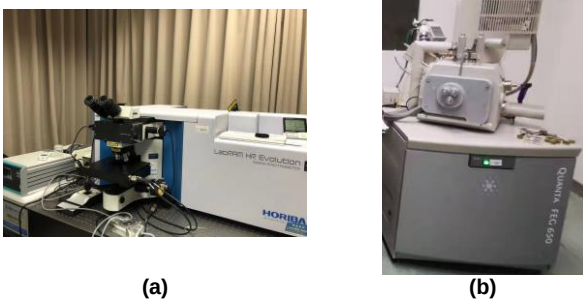

(a) (b)

Figure 2. Equipment used in the experiments (a)Raman spectroscopy (b)scanning electron microscope

2.5 Titration method

The proportion of corrosion products filling into cement paste of concrete block CHCD0 was determined by titration method. The whole process can be divided into two steps.

The first step was preparing samples for titration. There were no crack on the concrete surface. The concrete block CHCD0 was cut into 18 pieces with size of 83mmx100mmx50mm, the cutting line was shown in Figure 3a. The label A, B, C correspond to the three steel bars in concrete block, respectively. In each piece, there is a segment of steel bar. Then, the 18 pieces were carefully cut along the central axis to make the two parts of concrete and one segment of steel bar separate, as shown in Figure 3b. After cutting, the steel-concrete interfaces of concrete parts and steel bar segments were subjected to acid pickling, thus the corrosion products that induced volume expansion could dissolve into acid solution and form liquid samples for further titration. After acid pickling, the concrete parts were crushed and grinded into concrete powders for titration. Obviously, the corrosion products that filled into cement paste were included in those concrete powders. The residual steel bar segments were subjected to alkaline wash for preventing further corrosion. Each steel bar segment was weighed to obtain the residual mass. The whole process of sample preparation was shown in Figure 4.

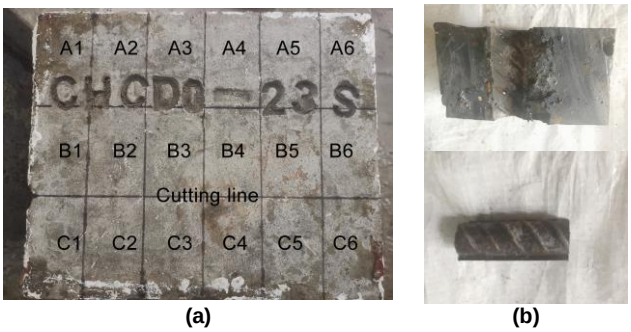

(a) (b)

Figure 3. Cut process of sample preparation (a)cutting line on concrete block (b)seperated concrete parts and steel bar segment of each piece

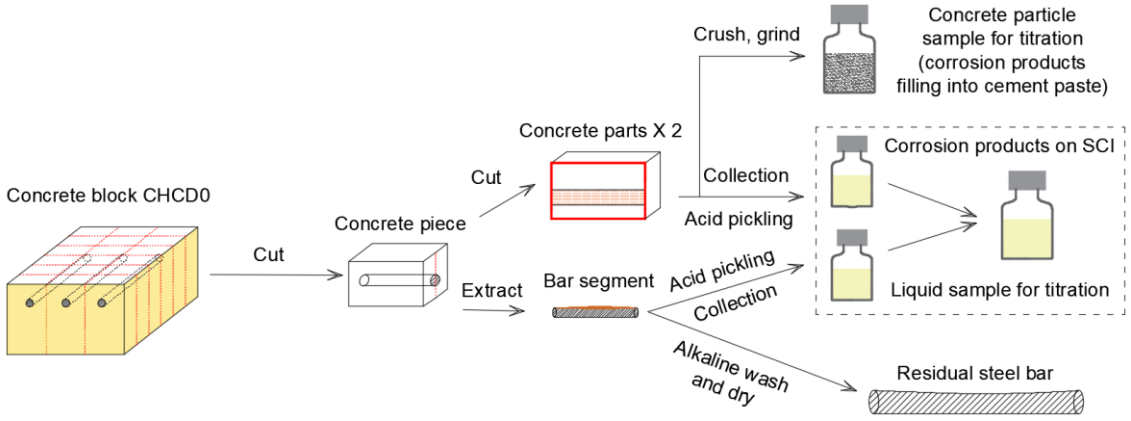

Figure 4. Process of sample prepration

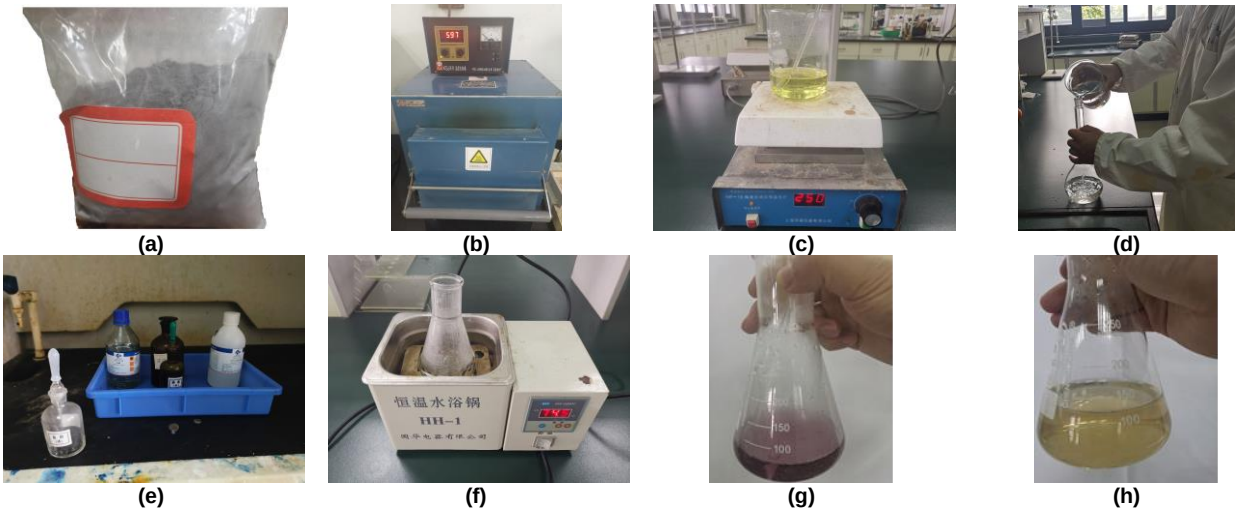

Figure 5. Process of titration (a)concrete powder (b)muffle furnace (c)leaching out dissolved in HCl and HNO3 (d)bring to volume (e)adjust PH in fume hood (f)heat in water bath for titration (g)add sodium sulfosalicylate to sample solution before titration (h)titration end point

The second step was titration method. As shown in Figure 5, EDTA titration method was used to determine the Fe content in liquid samples and concrete particle samples. The detailed steps were listed as follow (GB/T 176-2017) [12].

1) 30mL of 30% H_2O_2 and 10mL of 5M HCL were added to each liquid sample and mixed thoroughly. This step was necessary for the reason that the ferrous in corrosion products could be oxidized to ferric ion, enabled all corrosion products can be taken into consideration in the further titration. After vacuum filtration, the liquid sample was transferred to a 500-ml volumetric flask and bring to volume by distilled water. By this way, the solution T1 was ready for titration.
2) Approximately 0.5g concrete powders were weighed from each powder sample. The powders were put into silver crucible and mixed with 6g sodium hydroxide. The silver crucible was put into muffle furnace and heated to be fused for 20 minutes. The crucible was taken out and carefully put into a beaker containing 100mL boiling water for heating. After leaching out, the frits were flushed by distilled water, followed by mixing with 25mL of 10M HCl and 1mL of 10M HNO_3. The mixed solution was heated to boiling for 1 minute. After cooling down to room temperature, the solution was transferred to a 500-ml volumetric flask and bring to volume by distilled water. By this way, the solution T2 was ready for titration.
3) 5mL solution from T1 or 50mL solution from T2 was pipetted to a beaker, and then diluted to 100mL by adding distilled water. Ammonium hydroxide and HCl were used to adjust the PH of sample solution to 1.8, precise PH test strips were adopted as indicator. The sample solution

was then heated to 70 degrees Celsius in water bath. Ten drops of sodium sulfosalicylate added into the sample solution as indicator (showing purple color). The titration was carried out with 0.015mol/L EDTA solution until the luminous yellow color of Fe $[EDTA]_3$ complex appeared

3. Results

3.1 Chemical composition of the solution in simulated aggressive environment

The spectra of the solution in simulated aggressive environment was shown in Figure 6. Even with a high background, a band at ~1060cm^{-1} was discernible. This band can be attributed to CO_3^{2-} [13]. Another band at ~740cm^{-1} was due to the formation of β-FeOOH (akageneite), which had been detected by Raman spectroscopy in preceding research [14].

As mentioned before, the solution used to simulate the aggressive environment for mortar blocks are consisted of deionized water and analytically pure sodium chloride. As a result, only the H_2O molecules could be detected by Raman spectroscopy (sodium ion and chloride ion are monatomic ions and could not be detected by Raman Spectroscopy without special handling). It is known that the H_2O is characterized by a peak at ~3400 cm^{-1} with large half width, and hence not shown in Figure 6. The band of CO_3^{2-} originating from dissolved carbon dioxide in the atmosphere is reasonable because the container shown in Figure 7 is vented to the atmosphere. Besides, the β-FeOOH (akageneite) is not inherently in the solution, and must have come from the substances transfer at the interface of mortar blocks and solution.

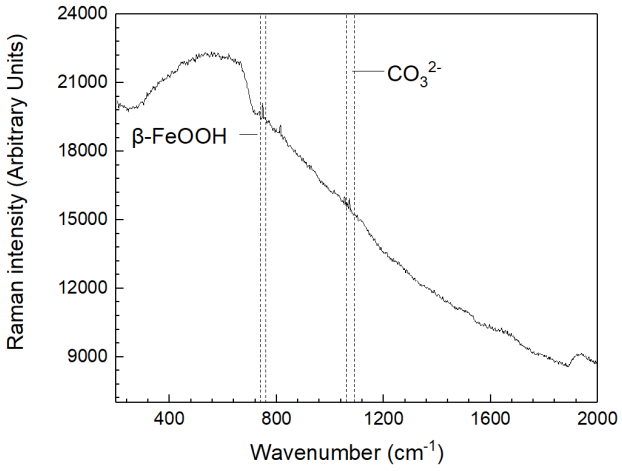

Figure 6. Raman spectra of the solution in simulated aggressive environment

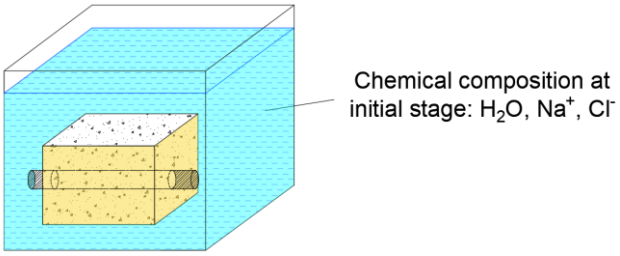

Figure 7. Chemical composition of solution in simluated aggressive enviroment

3.2 Chemical constituents and micromorphology of corrosion products at steel-concrete interface

The steel bars extracted from the mortar blocks are shown in Figure 8. It can be seen that there is no corrosion-induced crack on surface of mortar blocks, and the distribution of corrosion products is non-uniform and the radius loss of the steel bar is relatively low.

Many kinds of corrosion products can be seen in each sample. FE-SEM inspection shows very large aggregates of ferrihydrite particles as shown in Fig 9a. Due to the high absorption and surface activity ferrihydrite can be easily transformed to goethite or hematite by dissolution-recrystallization, especially in oxygen-rich environment [15]. A small population of needle-like goethite with sharp edge is shown in Fig 9b and large amounts of platelet-like hematite is shown in Fig 9c. That's because the corrosion products samples have been dried, leading to some of the ferrihydrite transformed to goethite and hematite. Besides, in the heated condition (~90 degrees Celsius), the ferrihydrite tends to transform to the α-Fe2O3 particles of a much less defined geometrical shape [16]. Shuttle-shaped Akageneite [17] can be seen in Fig 9d, which is in line with the Raman spectroscopy results. This kind of corrosion products only form in the chloride-rich environment due to the presence of chloride ion, which consist tunnel structure with FeOOH [18].

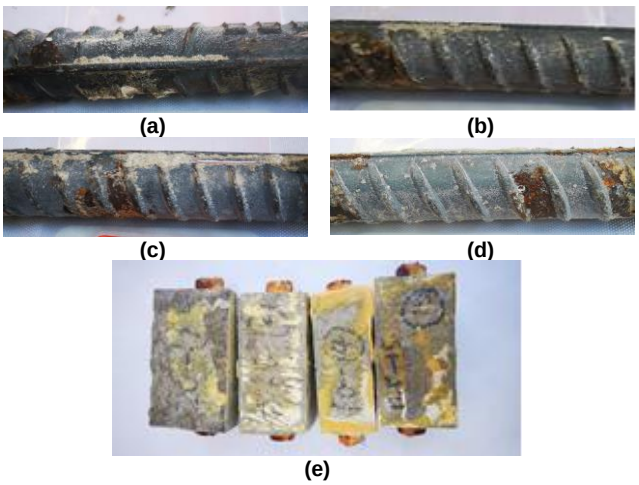

Figure 8. Mortar blocks(a)M-0.5-10 (b)M-0.5-15 (c)M-0.65-15 (d)M-0.5-20 (e)blocks after wet-dry cycle

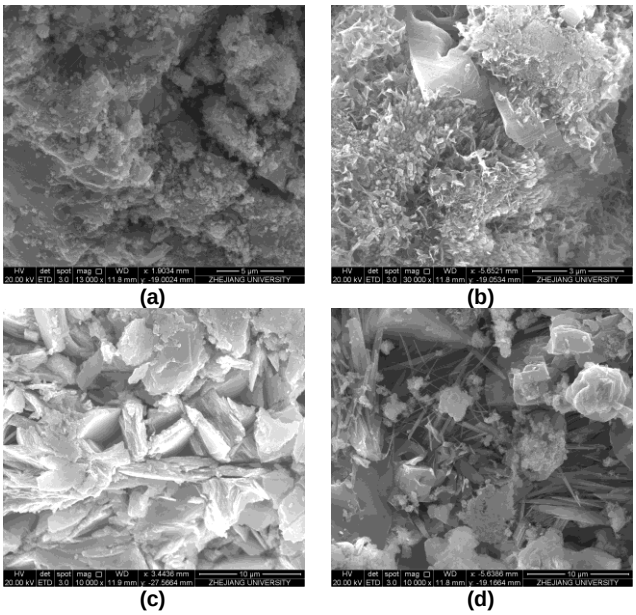

Figure 9. SEM image of corrosiosn products (a)ferrihydrite (b)goethite (c)hematite (d)akaganeite

3.3 Titration results and proportion of corrosion products filling into cement paste

The titration results of the solution T1, which represents all of the corrosion products adhere to the surface of steel bar and steel-concrete interface, is shown in Table 4. The titer of Fe(Ⅲ) (the equivalent mass of titrated substance when one millimeter of EDTA standard solution is consumed) T_{Fe} can be expressed as follows:

$$T_{Fe}=c(EDTA)\times 55.8422 \quad (1)$$

where c(EDTA) is the concentration of EDTA solution used in titration. Then, the mass of ferric and ferrous ion consisting of corrosion products dissolve in acid pickling as described in section 2.5 can be calculated. Considering the density of the steel (7.85g/cm^3) and length of the steel bar (5cm) in each piece cut from the concrete block CHCD0-23S, the mass of steel bar can be calculated as 78.92g. Therefore, the proportion of corrosion products inducing volume expansion at steel-concrete interface to the whole steel bar can be obtained as shown in Figure 10. It can be seen that the proportion of corrosion products of most of the pieces is concentrated in a small range between 0.1%-0.3% excepet piece A1 and C6. This phemonenon can be explained by the position of steel bar in A1 and C6, which is the most close to the concrete cover surface. Besides, particial failure of anti-corrosion precaution might occur at the adjacent place. As a result, the steel bar in A1 and C6 suffer from more severe corrosion.

The titration results of the solution T2, which represents parts of the corrosion products filling into cement paste, including pore, crack and crevice in concrete, is shown in Table 5. Compared to the solution T1, the data processing is different for solution T2. Firstly, the liquid sample containing solution T1 includes all of the corrosion products that induces volume expansion on steel-concrete interface. But the solution T2 is obtained by processing part of the particle sample as shown in Figure 4. Secondly, there are also a certain amount of Fe_2O_3 in cement, sand and coarse aggregate inherently, which interfer the titration of the corrosion products filling into the cement paste.

Therefore, the Fe(Ⅲ) in solution obtained from the titration is multiplied by the ratio of liquid sample T2 to solution for titration firstly. Then, the mass of Fe is divided by the mass of the approximately 0.5g concrete powers extracted from the particle (Figure 5a), and the Fe proportion in concrete can be obtained as shown in the last column of Table 5. However, the Fe proportion calculated in Table 5 includes both the corrosion products filling into cement paste and the inherent Fe_2O_3 in cement, sand and coarse aggregate, and the latter should be removed by substracting the Fe proportion measured in pure concrete powder sample as shown in the last row of Table 5. Therefore, the corrosion products filling into cement paste can be obtained as shown in Figure 11.

Table 4. Titration results of liquid sample (includes all of the corrosion products that induce volume expansion at steel-concrete interface)

Label of pieces	Volume of liquid sample T1 (mL)	Volume of solution for titration (mL)	EDTA consumption (mL)	Concentration of EDTA solution (mol/L)	Fe(Ⅲ) in solution (mg)	The mass of steel bar in pieces (g)
A1			6.51		3.64	
A2			2.15		1.20	
A3			2.35		1.31	
A4			2.7		1.51	
A5			2.32		1.30	
A6	500	5	1.6	0.01	0.89	78.92
B1			1.22		0.68	
B2			1.52		0.85	
B3			1.86		1.04	
B4			1.74		0.97	
B5			1.78		0.99	

B6	1.89	1.06
C1	3.14	1.75
C2	3.25	1.81
C3	2.1	1.17
C4	1.82	1.02
C5	1.11	0.62
C6	11.98	6.69

Table 5. Titration results of powder sample (includes parts of the corrosion products that fill into cement paste)

Label of pieces	Volume of liquid sample T2 (mL)	Volume of solution for titration (mL)	EDTA consumption (mL)	Mass of the concrete pieces (g)	Mass of the powder for making solution T2 (g)	Fe(Ⅲ) in solution (mg)	Fe proportion in concrete (%)
A1	500	50	1.31	1496	0.58	0.73	1.26
A2			1.23	1445	0.554	0.69	1.24
A3			1.15	1498	0.527	0.64	1.22
A4			1.13	1489	0.512	0.63	1.23
A5			1.17	1478	0.53	0.65	1.23
A6			1.21	1516	0.552	0.68	1.22
B1			1.29	1230	0.589	0.72	1.22
B2			1.15	1233	0.531	0.64	1.21
B3			1.36	1243	0.625	0.76	1.22
B4			1.36	1254	0.613	0.76	1.24
B5			1.33	1238	0.608	0.74	1.22
B6			1.18	1267	0.533	0.66	1.24
C1			1.21	1510	0.557	0.68	1.21
C2			1.08	1491	0.495	0.60	1.22
C3			0.96	1514	0.441	0.54	1.22
C4			1.21	1509	0.552	0.68	1.22
C5			0.94	1504	0.433	0.52	1.21
C6			1.24	1525	0.56	0.69	1.24
Pure concrete			1.14	1518	0.527	0.64	1.21

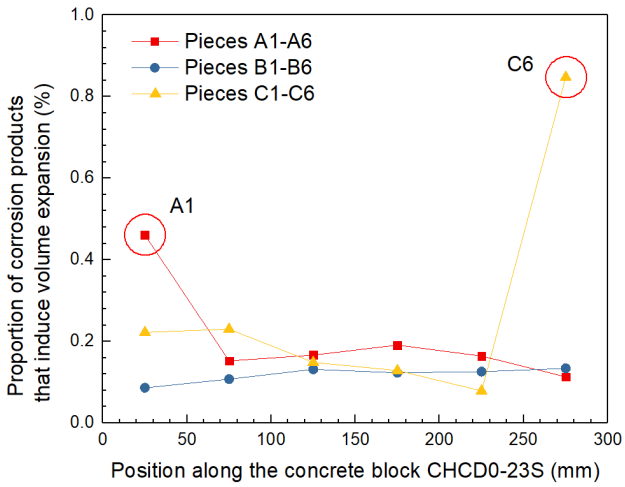

Figure 10. The proportion of corrosion products inducing volume expansion at steel-concrete interface to the whole steel bar

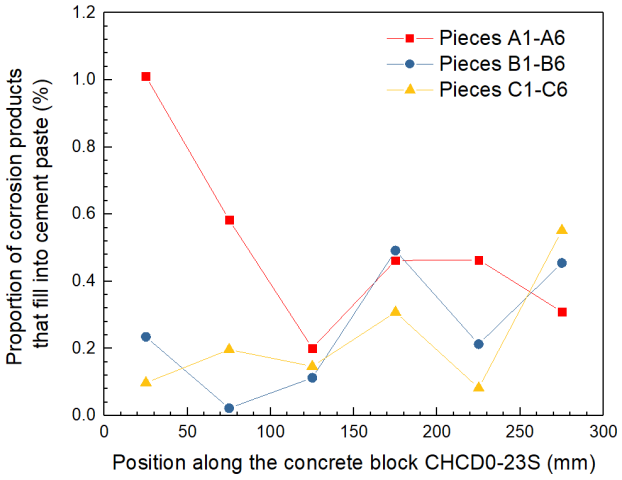

Figure 11. The proportion of corrosion products filling into the cement paste to the whole steel bar

4. Discussion

4.1 Mechanisms of corrosion products filling

According to the experimental results, the corrosion products adhering to the surface of steel bar and at the steel-concrete interface are consisted of hematite (α-Fe_2O_3), goethite (α-FeOOH), akageneite (β-FeOOH) and ferrihydrite. And akageneite (β-FeOOH) is also detected in the solution where the mortar blocks immerse, indicating that some corrosion products transport from steel-concrete interface to the solution outside the blocks.

Besides, If the corrosion products transportation was in solid phase and carried by water flow, the goethite and hematite in solid phase would be driven and flow to the external solution. Therefore, this hypothesis is proved to be false. The mechanisms of corrosion products transportation can be deduced as ion diffusion when there is no crack propagating through the concrete cover.

It should be noted that there is no direct evidence to prove the diffusion mechanism, and the predominant problem is the form of corrosion products during the diffusion process. According to the solubility of corrosion products, the diffusion rate should be extremely low (the akageneite has the highest solubility in alkaline or neutral environment among those four kinds of corrosion products found by FE-SEM). In contrast, it only takes 9-months for corrosion products transport from steel-concrete interface to external solution, diffusing through at least 10 mm. This contradictions between theory and actual phenomenon imply that the akageneite is not the substance that control the diffusion process, and there might be some Fe-containing complex with high solubility in the cement or concrete. This kind of substance might be unstable that can not be detected after disengaging from the simulated aggressive environment [19].

In general, the corrosion products in the form of unstable Fe-containing complex dissolve in the pore solution, then diffuse towards the surface of mortar of concrete block through the pore solution, and then precipitate when the condition changes, finally are observed in the cement paste as filling corrosion products in solid phase. Further studies are needed to determine the intermediate state of corrosion products when diffusing in pore solution through the mortar or concrete.

4.2 Filling capacity of corrosion products

Based on Figure 10 and Figure 11, the proportion of corrosion products inducing volume expansion and corrosion products filling into cement paste can be obtained as shown in Figure 12. The proportion of corrosion products filling into cement paste is labelled upon the top of the bar. Over half of the pieces cut from concrete block show high filling capacity of corrosion products (over 50% of all). Compared to the results of preceding research [18], where the proportion of corrosion products filling into cement paste to all of the corrosion products is 23%-33%, the filling proportion obtained from this study is obviously higher. This difference can be explained by the applied test method. In preceding study [20], only the regions at the adjacent of steel-concrete interface are investigated by FE-SEM, thus the corrosion products transport in distant cement paste can not be detected. Besides, only the corrosion products exceeding a certain volume can be detected. Furthermore, the scattered data extracted from several 2D planes (at different section of concrete specimen) is not representative. As a result, the corrosion products filling into cement paste might be underestimated. Whereas in this study, all of the concrete block is cut, crushed, grinded and collected, so all of the corrosion products can be included.

It can also be seen that even in the same concrete block, the corrosion products show different filling capacity at different parts. This can be due to the heterogeneity of concrete. There are many pores with different sizes and shapes in concrete as well as different types of coarse aggregates. The former has negative effects of concrete permeability, and the latter has positive effects of concrete permeability, which reduces the ingress and movement of fluid media [21]. In order to establish applicable models for predicting the proportion of corrosion products filling into cement paste, future studies should be done to explore the influencing factors on corrosion products transportation such as concrete cover thickness, water-cement ratio or pre-crack, etc.

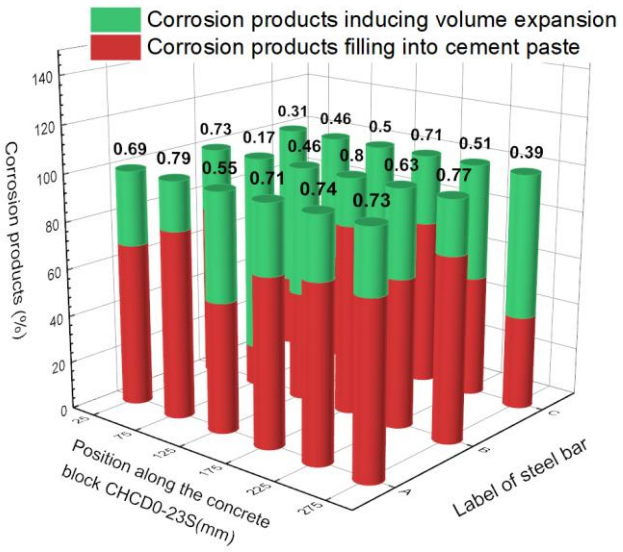

Figure 12. The proportion of corrosion products filling into the cement paste and corrosion products inducing volume expansion

5. Conclusion

In this study, the chemical components, micromorphology and transportation of corrosion products in mortar and concrete are investigated, and the followed conclusion can be drawn:

(1) The corrosion products adhering to steel bar surface and those at the steel-concrete interface are composed of goethite, akageneite, hematite and ferrihydrite.

(2) In wet-dry cycle condition, the corrosion products in cementitious material would transport to the external chloride-rich environment and transform to akageneite.

(3) The proportion of corrosion products filling into cement paste is underestimated by simply detecting the region in the adjacent of steel-concrete interface.
(4) Disassembling the concrete block, extracting the corrosion products in different parts and using EDTA titration method provide an effective way for quantifying the filling and transportation of corrosion products.

REFERENCES

1. Bazant, Z.P., 1979. Physical model for steel corrosion in concrete sea structures—application. J. Struct. Div, 105 ASCE 14652 Proceeding.
2. Lin, X., Peng, M., Lei, F., Tan, J., Shi, H., 2017. Analytical model of cracking due to rebar corrosion expansion in concrete considering the structure internal force. AIP Advances, 7(12):125328.
3.Angst, U., Elsener, B., Jamali, A., Adey, B., 2012. Concrete cover cracking owing to reinforcement corrosion – theoretical considerations and practical experience. Materials and corrosion, 63(9999).
4. Liu, Y., 1996. Modeling the Time-to-Corrosion Cracking in Chloride Contaminated Reinforced Concrete Structures. Doctoral dissertation.
5. Caré, S., Nguyen, Q.T., L'Hostis, V., Berthaud, Y., 2008. Mechanical properties of the rust layer induced by impressed current method in reinforced mortar. Cement and Concrete Research, 38(8-9): 1079-1091.
6. Nguyen, Q.T., Millard, A., Caré, S., L'Hostis, V., Berthaud, Y., 2006. Fracture of concrete caused by the reinforcement corrosion products. Journal De Physique IV, 136:109-120.
7. Michel, A., Pease, B.J., Geiker, M.R., Stang, H., Olesen, J.F., 2011. Monitoring reinforcement corrosion and corrosion-induced cracking using non-destructive x-ray attenuation measurements. Cement & Concrete Research, 41(11):1085-1094.
8. Zhao, Y.X, Ding, H.J., Jin, W.L., 2014. Development of the corrosion-filled paste and corrosion layer at the steel/concrete interface. Corrosion Science, 87:199–210.
9. Yu, J., 2011. Damage analysis and experimental study of reinforced concrete structures with rebar corrosion (in Chinese). Zhejiang University, Doctoral dissertation.
10. Melchers, R.E., Li, C.Q., 2009. Reinforcement corrosion in concrete exposed to the north sea for more than 60 years. Corrosion, 65(8): 554-566.
11. Cornell, R.M., Schwertmann, U., 1996. The iron oxides.
12. GB/T 176-2017. Methods for Chemical Analysis of Cement. General Administration of Quality Supervision, Inspection and Qurantine of the People's Republic of China.
13. SI, G., Yang, D., Guo, J., Liu, Q., Ye, W., Zheng, R., 2019. Optimization of a near-concentric cavity Raman spectroscopy system for liquid sample and preliminary results of $CO3_{2^-}$/HCO_{3^-} (in Chinese). Spectropy and Spectral Analysis, 39(4): 1086-1091.
14. Boucherit, N., Goff H. A., Joiret, A., 1991. Raman studies of corrosion films grown on Fe and Fe-6Mo in pitting conditions. Corrosion Science, 32(5-6): 497-507.
15. Yang, Z., Zeng, X., Sun, B., Bai, L., Su, S., Wang, Y., Wu, C., 2020. Research progress on the stability of ferrihydrite structure and its application in arsenic fixation (in Chinese). Journal of Agro-Environment Science, 39(3): 445-453.
16. Žic, M., Ristić, M., Musić, S., 2007. 57Fe Mössbauer, FT-IR and FE SEM investigation of the formation of hematite and goethite at high pH values. Journal of Molecular Structure, 834, 141-149.
17. Li, M., Li, B., Meng, F., Liu, J., Yuan, Z., Wang, C., & Liu, J., 2018. Highly sensitive and selective butanol sensors using the intermediate state nanocomposites converted from β-FeOOH to α-Fe2O3. Sensors and Actuators B: Chemical, 273, 543-551.
18. Réguer, S., Mirambet, F., Rémazeilles, C., Vantelon, D., Kergourlay, F., Neff, D., & Dillmann, P., 2015. Iron corrosion in archaeological context: Structural refinement of the ferrous hydroxychloride β-Fe2 (OH) 3Cl. Corrosion Science, 100, 589-598.
19. Sagoe-Crentsil, K. K., Glasser, F.P., 1993. "Green rust", iron solubility and the role of chloride in the corrosion of steel at high pH. Cement & Concrete Research, 23(4):785-791.
20.Faris, G.W., Copeland, R. A., 1997. Wavelength dependence of the Raman cross section for liquid water. Applied Optics, 36(12):2686-8.
21.Zhang, M. H., Hui, L., 2011. Pore structure and chloride permeability of concrete containing nano-particles for pavement. Construction & Building Materials, 25(2), 608-616.